Geochemistry Geophysics Geosystems G3
AN ELECTRONIC JOURNAL OF THE EARTH SCIENCES
Published by AGU and the Geochemical Society

Article
Volume 10, Number 6
25 June 2009
Q06017, doi:10.1029/2009GC002486
ISSN: 1525-2027

A 2 Ma record of explosive volcanism in southwestern Luzon: Implications for the timing of subducted slab steepening

Yueh-Ping Ku
Department of Geosciences, National Taiwan University, Taipei 106, Taiwan

Now at Institute of Environmental Engineering, National Chiao Tung University, No.1001, University Road, Hsinchu 30010, Taiwan (d90224003@ntu.edu.tw)

Chang-Hwa Chen
Institute of Earth Sciences, Academia Sinica, Taipei 11529, Taiwan

Sheng-Rong Song
Department of Geosciences, National Taiwan University, Taipei 106, Taiwan

Yoshiyuki Iizuka and Jason Jiun-San Shen
Institute of Earth Sciences, Academia Sinica, Taipei 11529, Taiwan

[1] New chemical and isotopic analyses of the tephra layers plus deep-sea tephrostratigraphic record from two cores from either side of Luzon Island (Philippines) have allowed the identification of two periods of explosive volcanic activity originating from the Macolod Corridor in the southwestern part of the Luzon. The first period extended from prior to 1355 ka to 1977 ka, and the second period extended from 478 ka to the present, separated by a period of relative quiescence. The time intervals between large explosive eruption events in each period were 31 ± 15 ka and 156 ± 52 ka, respectively. Combined with published chronological and geochemical data from onshore volcanic deposits, the tephrostratigraphic record shows that the locus of large explosive eruptions has migrated southwestward from the northeastern section to the middle and southwestern sections of the Macolod Corridor. The period of relative quiescence is characterized by monogenetic volcanism in the central section of the corridor. The migration of active volcanism across the southwestern part of Luzon during the Quaternary is used to infer the evolution of the subducting South China Sea crust. The period of relative quiescence represents a period of adjustment of the subducted slab by steepening, which began around 1355 ka or shortly thereafter and finished at around 478 ka.

Components: 12,136 words, 10 figures, 2 tables.

Keywords: tephrostratigraphy; explosive eruption; Luzon; Philippine; subducted slabs.

Index Terms: 8455 Volcanology: Tephrochronology (1145); 8428 Volcanology: Explosive volcanism; 8413 Volcanology: Subduction zone processes (1031, 3060, 3613, 8170).

Received 9 March 2009; **Revised** 4 May 2009; **Accepted** 15 May 2009; **Published** 25 June 2009.

Ku, Y.-P., C.-H. Chen, S.-R. Song, Y. Iizuka, and J. J.-S. Shen (2009), A 2 Ma record of explosive volcanism in southwestern Luzon: Implications for the timing of subducted slab steepening, *Geochem. Geophys. Geosyst.*, *10*, Q06017, doi:10.1029/2009GC002486.

1. Introduction

[2] The alignment of active volcanoes above a subduction zone generally takes the form of one or two chains that lie parallel to the trench. Such an alignment of active volcanoes in an island arc setting may help to infer the geometry of the subducted slab because of the specific depth of dehydration and the subsequent melting of the overlying mantle [*Tatsumi and Eggins*, 1995]. Therefore, the recognition of geographic shifts in the distribution of arc volcanism may help to elucidate the changing geometry of a subducted slab in the region of interest.

[3] For Luzon Island in the Philippines (Figure 1), the long-term evolution of the slab underlying the volcanic arc along its western edge and the general tectonic configuration of the region are reasonably well documented [*Cardwell et al.*, 1980; *Hamburger et al.*, 1983; *Bautista et al.*, 2001]. Luzon Island lies to the east of the Manila Trench, along which the South China Sea crust is subducting eastward beneath the island [*Bautista et al.*, 2001]. The southwestern part of the island is located near the southern end of the Manila Trench. The Macolod Corridor, an active Quaternary volcanic area in this part of the island, is aligned southwest to northeast, i.e., at a right angle to the Manila Trench. In this respect, the corridor is distinguished from other active volcanic areas of Luzon Island including the North Luzon, Bataan, and Mindoro Segments, all of which are aligned in one or two chains parallel to the Manila Trench (Figure 1). The southward extension of the Trench terminates in a suture zone that is the result of the collision of the North Palawan Continental Terrane and the Philippine Mobile Belt, which began in the Early Miocene [*Marchadier and Rangin*, 1990]. In southern Luzon, the Bicol Arc is related to westward subduction of the Philippine Sea Plate along the Philippine Trench (Figure 1).

[4] The Macolod Corridor is composed of two calderas, three stratovolcanoes, and hundreds of maars and scoria cones. On the basis of the spatial configuration and ages of volcanic rocks in the corridor, *Oles* [1991] suggested that the locus of active volcanism during the Quaternary migrated southwestward. *Sudo et al.* [2000] subsequently proposed that the start of the migration of the active volcanic area should lie between 1.6 Ma and 1.0 Ma, and that the migration was accompanied by a steepening of the subducted slab beneath southwestern Luzon Island.

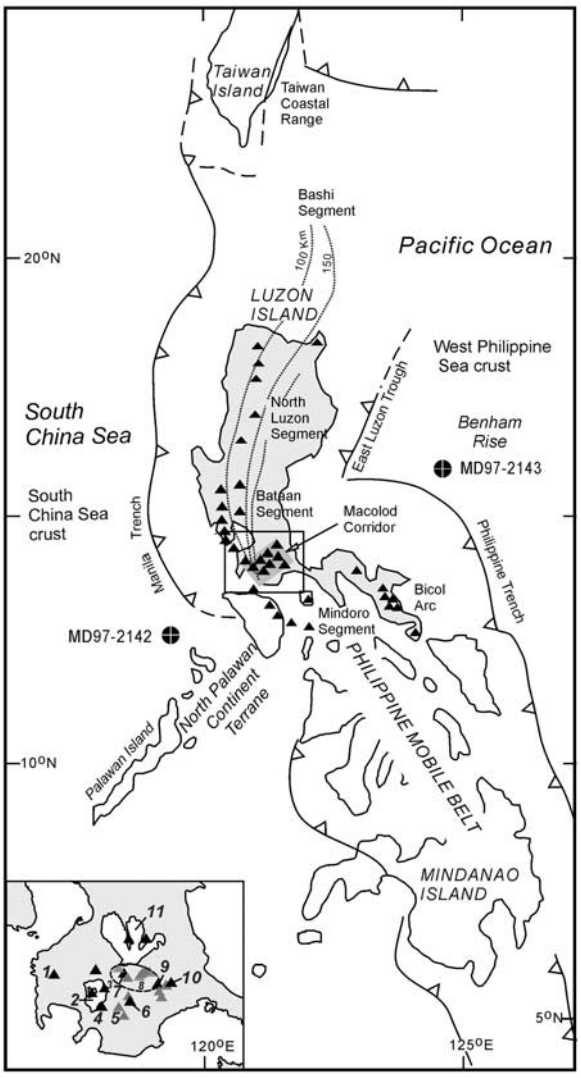

Figure 1. Quaternary volcanoes of Luzon Island, modified from *Defant et al.* [1989] and *Sudo et al.* [2000], along with the locations of the two deep-sea cores. Solid triangles denote Quaternary volcanoes (gray triangles denote monogenetic volcanoes); dashed lines denote the tops of Benioff zones; crosses in circles denote positions of deep-sea cores. Numbers are as follows: 1, Mount Palay-Palay, Mount Batulao; 2, Taal Lake Caldrea; 3, Mount Sungay; 4, Mount Macolod; 5, Anilao Hill; 6, Mount Malepunyo; 7, Mount Makiling; 8, Maar Field; 9, Mount San Cristobal; 10, Mount Banahaw; 11, Laguna de Bay Caldera area.

[5] Trace element studies of Quaternary volcanic rocks suggests that the Laguna de Bay Caldera, located in the northeastern part of the Macolod Corridor (Figure 1), formerly lay above the subducted slab [*Oles*, 1991; *Knittel and Oles*, 1995]. Indeed, seismic data indicate that at present, this northeastern part of the corridor is no longer located above the slab [*Bautista et al.*, 2001].

Seismic data also indicate that a near-vertical subducted slab, traceable to a depth of 300 km, lies beneath the Taal Lake Caldera located in the southwestern part of the corridor [*Bautista et al.*, 2001] (Figure 1). Although this Quaternary geodynamic adjustment of the subducted slab under the corridor has been broadly constrained, more geochronological data are required if a robust characterization and understanding of the geodynamic evolution of the subducted slab is to be established.

[6] This study presents two deep-sea tephrostratigraphies from cores taken offshore to the east and west of Luzon Island that provide a more complete and refined record of the explosive eruptive history of the Macolod Corridor during the Quaternary than has been previously available. Combining deep-sea tephrostratigraphies with available data for onshore volcanic rocks in the corridor leads to a better characterization of the timing and spatial configuration of the southwestward migration of the locus of active volcanism along the corridor. This characterization translates into a more precise chronology of the steepening of the slab under southwestern Luzon Island.

2. Southwestern Luzon Island: Volcanic Province and Tectonic Setting

[7] Luzon Island includes two volcanic arcs, the Luzon Arc and the Bicol Arc. The Luzon Arc, from north to south, comprises six volcanic segments (Figure 1): the Taiwan Coastal Range, the Bashi Segment, the North Luzon Segment, the Bataan Segment, the Macolod Corridor, and the Mindoro Segment [*Yang et al.*, 1996]. The Quaternary volcanic rocks in the southernmost four segments, from north to south, have increasing K_2O contents and Sr isotopic ratios (Figures 2 and 3) [e.g., *Knittel and Defant*, 1988] due to the collision of the North Palawan Continental Terrane and the Philippine Mobile Belt in the central Philippines and the resulting probable involvement of continental material in the magma genesis.

[8] The Macolod Corridor [*Defant et al.*, 1988; *Förster et al.*, 1990] is characterized by a dense distribution of eruptive volcanic centers aligned in a 40-km-wide belt perpendicular to the Manila Trench, and it lies parallel to the current direction of the Palawan Island extension (Figure 1) though this alignment may be coincidental. The corridor's southwestern end is marked by Taal Lake Caldera, a 26 × 25 km depression with a volume of around 120 km^3. From there, the corridor trends northeast, encompassing three stratovolcanoes and hundreds of monogenetic volcanoes (cones and maars). The corridor terminates in the northeast at the Laguna de Bay Caldera, a depression with three lobes covering an area of 41 × 36 km (Figure 1). The southwestern section of the corridor contains the Taal area, the middle section includes two stratovolcanoes (Mount Makiling and Mount Malepunyo) and hundreds of monogenetic volcanoes, and the northeastern section includes the area of the Laguna de Bay Caldera and several stratovolcanoes (Mount San Cristobal and Mount Banahaw).

[9] Volcanic rocks from the northeastern section of the corridor contain relatively higher K_2O contents (from calc-alkaline series to shoshonitic series) than those from the middle and southwestern sections (from calc-alkaline series to high-K series; Figure 2). The Sr isotopic ratios of volcanic rocks from the Macolod Corridor vary over a wide range, from 0.7041 to 0.7049 with only two samples out of 56 having higher ratios (Figure 3). The ratios are higher than those of the Bicol Arc (Figure 3), which is associated with the westward subduction of the western Philippine crust along the Philippine Trench (Figure 1), and also higher than those from the North Luzon Segment [*Knittel et al.*, 1995].

[10] Current knowledge of the tectonic environment in which the Quaternary volcanic rocks of the Macolod Corridor have formed has hitherto been constructed entirely from geochemical and chronological studies of on-land volcanic rocks [e.g., *Oles*, 1991; *Sudo et al.*, 2000]. These studies have included analyses of the major and trace element contents, isotopic compositions, K-Ar dating, and ^{14}C dating. Available isotopic ratios for Macolod Corridor volcanic rocks suggest that they contain components derived from subducted South China Sea crust and from sediments overlying the subducted crust [*Knittel and Defant*, 1988; *Knittel et al.*, 1988]. *Defant et al.* [1988] and *Knittel and Oles* [1995] have argued that some magmas were probably generated during rifting.

[11] On the basis of major and trace element analyses, it has been suggested that the volcanic rocks of the two calderas located at the extremities of the Macolod Corridor are products of subduction-related magmatisms [*Oles*, 1991; *Sudo et al.*, 2000]. The reported age for the volcanic rocks in the Taal Lake Caldera area is no older than 2.22 ± 0.10 Ma (Figure 4), while the ages of the Taal Lake Caldera tuffs are no older than 0.31 ± 0.18 Ma [*Oles*, 1991; *Sudo et al.*, 2000]. For the Laguna de

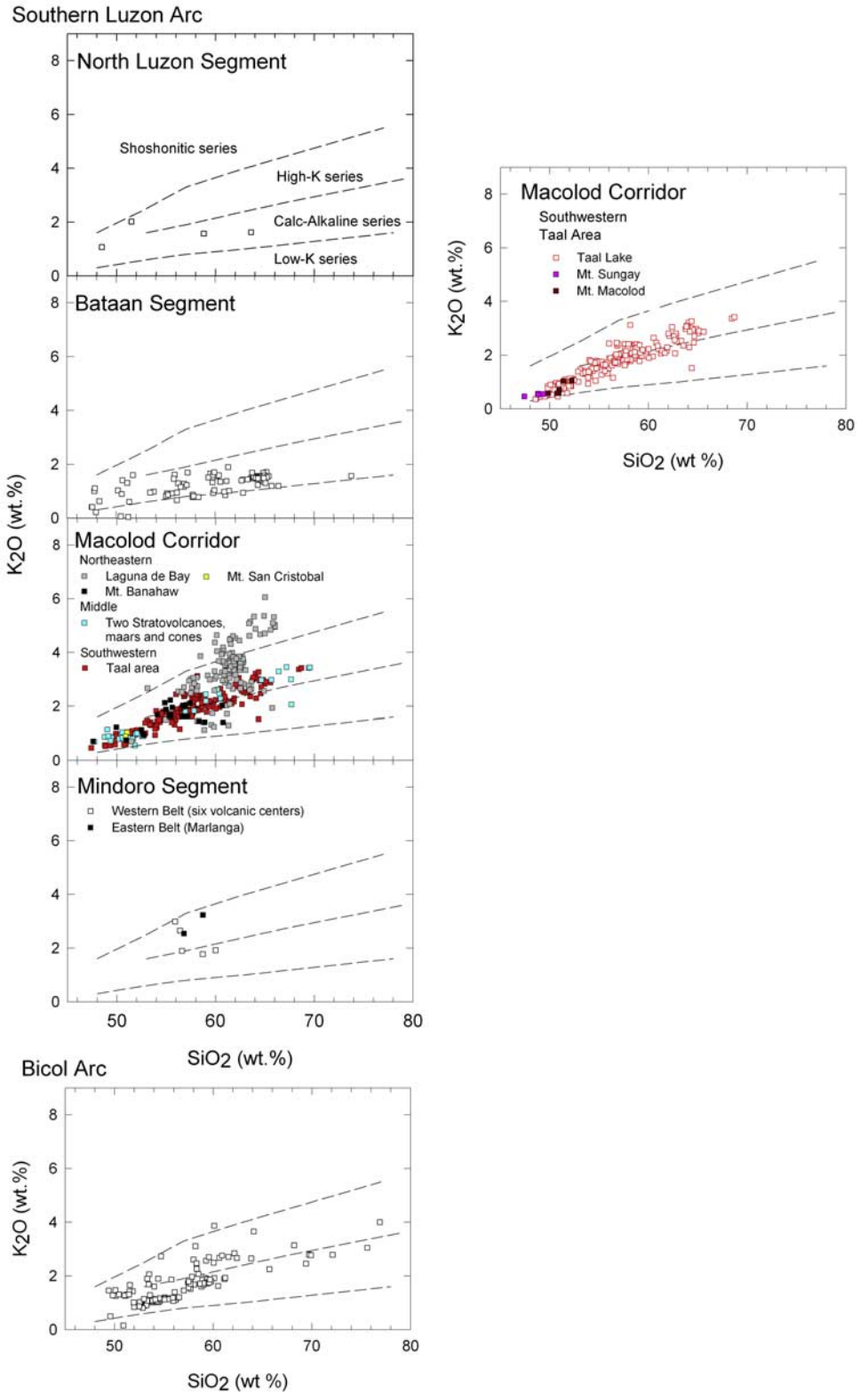
Southern Luzon Arc
North Luzon Segment
Shoshonitic series
High-K series
Calc-Alkaline series
Low-K series
Bataan Segment
Macolod Corridor
Northeastern
Laguna de Bay
Mt. San Cristobal
Mt. Banahaw
Middle
Two Stratovolcanoes, maars and cones
Southwestern
Taal area
Mindoro Segment
Western Belt (six volcanic centers)
Eastern Belt (Marlanga)
K2O (wt.%)
SiO2 (wt.%)
Macolod Corridor
Southwestern
Taal Area
Taal Lake
Mt. Sungay
Mt. Macolod
K2O (wt.%)
SiO2 (wt %)
Bicol Arc
K2O (wt.%)
SiO2 (wt %)

Figure 2

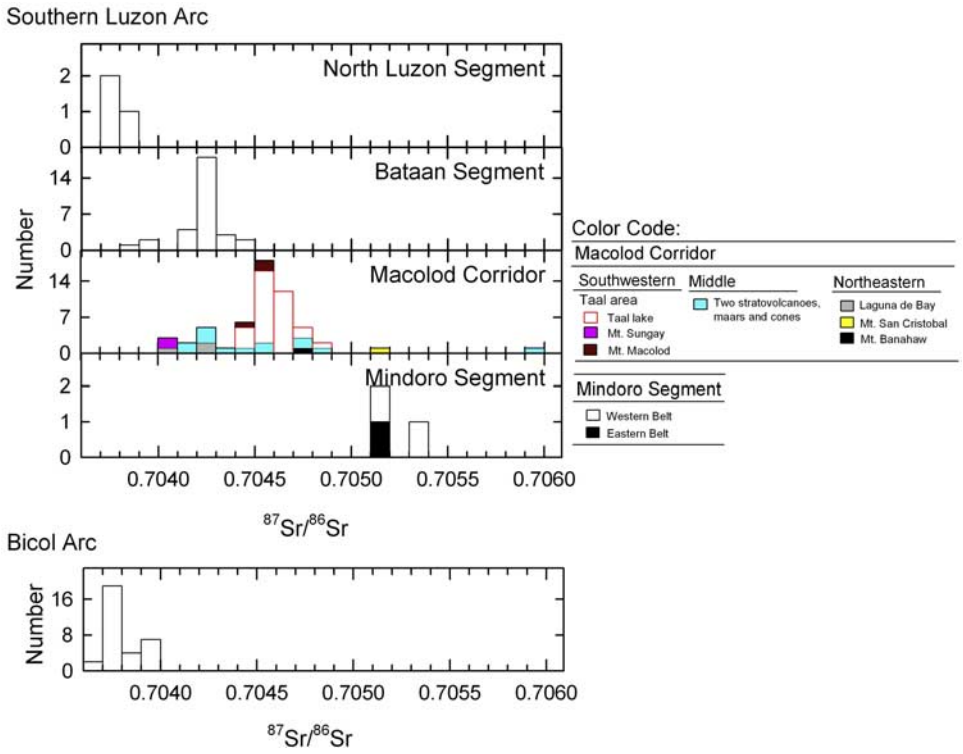

Figure 3. Sr ratios of Quaternary volcanic rocks of the Southern Luzon Arc and Bicol Arc. Data are from all available in the literature [*Defant and Ragland*, 1988; *Defant et al.*, 1988; *Knittel et al.*, 1988; Knittel and Defant 1988; *Defant et al.*, 1990; *Knittel-Weber and Knittel*, 1990; *Defant et al.*, 1991; *Delfin et al.*, 1993; *McDermott et al.*, 1993; *Mukasa et al.*, 1994; *Knittel and Oles*, 1995; *Bernard et al.*, 1996; *Castillo and Punongbayan*, 1996; *Knittel et al.*, 1997; *Castillo and Newhall*, 2004; *McDermott et al.*, 2005; *DuFrane et al.*, 2006].

Bay Caldera, the reported ages for lavas and tuffs lie between 1.6 Ma and 2.3 Ma (Figure 4), except for one tuff formation near Manila city, which is younger than 47 ka [e.g., *Oles*, 1991; *Sudo et al.*, 2000].

[12] In the area between the calderas, the trace element contents of the basaltic rocks from the monogenetic scoria cones possess geochemical and mineralogical signature suggesting their derivation from a MORB-type mantle modified by subduction, suggesting perhaps that they are the products of incipient back-arc basin magmatism [*Knittel and Oles*, 1995]. The K-Ar ages for the three stratovolcanoes and monogenetic volcanoes in the Macolod Corridor are all younger than 1.7 Ma (Figure 4) [e.g., *Oles*, 1991; *Sudo et al.*, 2000]. Some magmatism, represented by some domes on the flanks of the major stratovolcanoes, younger than 100 ka, appears to contain the signature of a newly forming continental crust [*Vogel et al.*, 2006].

3. Materials and Methods

[13] Two deep-sea giant piston cores from either side of Luzon Island, MD97-2142 and MD97-2143 (Figure 1), were used to investigate the Quaternary volcanic history of the Macolod Corridor. Site MD97-2142 (12°41.33′N, 119°27.90′E) is situated near the southern end of the Manila Trench in the South China Sea basin. Site MD97-2143

Figure 2. (left) Harker diagrams [*Rickwood*, 1989] for the Quaternary volcanic rocks of the Southern Luzon Arc and Bicol Arc. (right) The Quaternary volcanic rocks of the Taal area. The plotted data are from the available literature [*Divis*, 1980; *Wolfe and Self*, 1983; *Defant and Ragland*, 1988; *Defant et al.*, 1988; *Knittel and Defant*, 1988; *Defant et al.*, 1989, 1990; *Knittel-Weber and Knittel*, 1990; *Defant et al.*, 1991; *Miklius et al.*, 1991; *Delfin et al.*, 1993; *McDermott et al.*, 1993; *Listanco*, 1994; *Knittel and Oles*, 1995; *Bernard et al.*, 1996; *Castillo and Punongbayan*, 1996; *Luhr and Melson*, 1996; *Knittel et al.*, 1997; *Castillo and Newhall*, 2004; *Andal et al.*, 2005; *McDermott et al.*, 2005; *DuFrane et al.*, 2006; *Vogel et al.*, 2006].

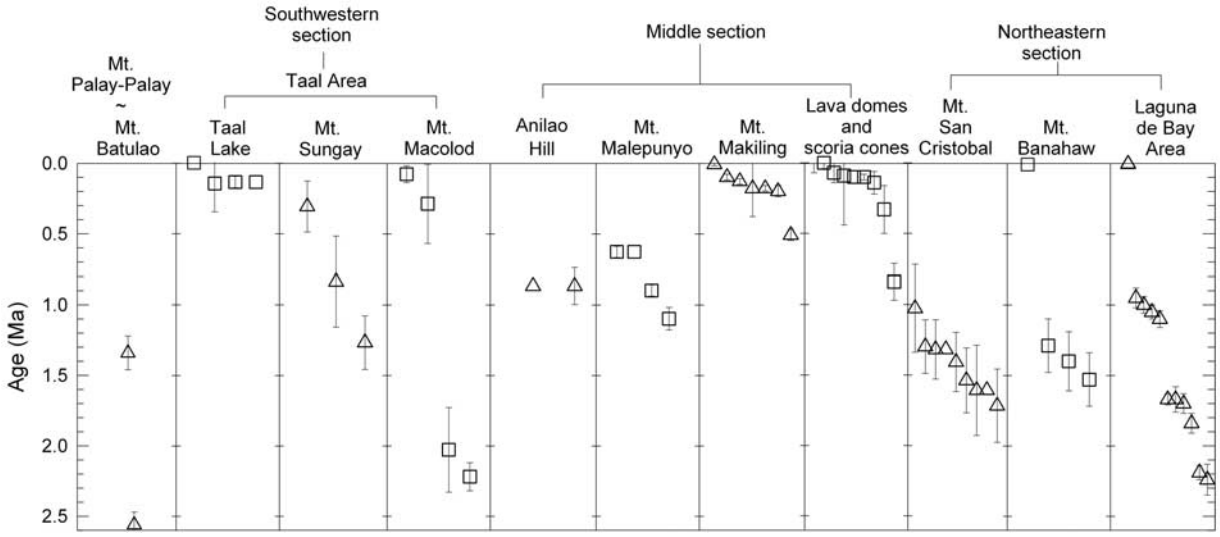

Figure 4. Available chronological data for active Quaternary volcanoes of southwestern Luzon Island. For the locations of these volcanoes, please refer to Figure 1. Data are shown with uncertainties of ±1 SD. Data sources: *de Boer et al.* [1980], *Wolfe* [1981], *Oles* [1991], *Listanco* [1994], and *Sudo et al.* [2000].

(15°52.262′N, 124°38.96′E) is located in the Benham Rise in the West Philippine Sea basin. These two deep-sea cores were taken at water depths of 1557 m and 2989 m, respectively, during the IMAGES III Leg II cruise in June 1997. The total recovered material lengths for the cores were 35.91 m and 37.95 m, respectively. The material from both cores consists of very fine grained hemipelagic sediments, silty clay, calcareous oozes, and intercalated tephra layers that consist of glass shards and minerals.

[14] According to the oxygen isotope age models for these two cores [*Horng et al.*, 2002; *Wei et al.*, 2003], their stratigraphic ages cover the past 870 ka in Core MD97-2142 and 2140 ka in Core MD97-2143. The age models were based on 72 chronological control points in Core MD97-2142 [*Wei et al.*, 2003] (Table 1) and 56 age control points that were further used to tune the astronomical age in Core MD97-2143 [*Horng et al.*, 2002]. The occurrence of tephra layers in these two cores has been previously reported by *Wei et al.* [1998], *Lee* [2000] and *Horng et al.* [2002]. Although geochemical analyses of the tephra layers and glass particles have already been performed [*Tsai*, 2000; *Huang*, 2003], there is still a lack of reliable geochemical data for the glass particles, and the implications of the occurrence of tephra layers in the two cores remain unexplored.

[15] In this study, the thickness of each tephra layer was defined from the apparent color and structural changes of the sediment sequence on the surface of the split cores. By assuming a constant sedimentation rate between two available age control points given by oxygen isotope stratigraphy of Core MD97-2142 [*Wei et al.*, 2003], or between two astronomical tuning ages at two depths given by oxygen isotope stratigraphy of Core MD97-2143 [*Horng et al.*, 2002] (Table 1), the depositional age for the tephra layer between two control points or two depths was calculated after subtracting the tephra layer thickness (Table 1). Uncertainty in the age calculations was less than 2 ka, given the uncertainty (<1 cm) in measuring the thickness of the tephra layers. Therefore, the tephra ages quoted in the text and reported in Table 1 should be regarded as having uncertainties on the order of ±2 ka.

[16] Each tephra layer identified in the two cores, except for those deposited in the deepest 8 m of Core MD97-2143, was processed to obtain the major element and Sr isotope compositions of their glass particle components (>125 μm). The major elements of the glass particles were analyzed with a JEOL JXA-8900R Electron Probe MicroAnalysis (EPMA) instrument using an accelerating voltage of 10–15 kV and a beam current of 5–10 nA with a beam diameter of <15 μm. Strontium was extracted from ~500 glass particles for each analyzed layer after dissolution using a Sr-Spec column. The Sr isotopic ratios of the glass particles were analyzed using a MAT-262 Thermal Ionization Mass Spectrometer (TIMS). The ratios were normalized to $^{86}Sr/^{88}Sr = 0.1194$. Repeated analyses of the NBS-987 standard gave a mean of 0.71023 ± 0.00004

Table 1 (Sample). Physical, Chemical, and Chronological Data for the Tephra Layers From the Two Deep-Sea Cores MD97-2142 and MD97-2143 [The full Table 1 is available in the HTML version of this article]

Core MD97-2142 Layer Nomenclature	Depth (m)	Thickness (cm)	Age Model for the Tephra Layer: Depth-Age Control Points[a] Near Each Tephra Layer: Upper Depth (m)	Upper Age (ka)	Lower Depth (m)	Lower Age (ka)	Estimated Age for Tephra Layer (ka)	Interval Depth (cm)	Mineral Assemblage[b]: Plagioclase	Quartz	Clinopyroxene	Orthopyroxene	Biotite
A	1.210	1.0	0.69	5	1.45	6	6	119–20	*		*		
B	4.740	1.0	4.25	34	6.01	52	39	473–74	*		*		
C	6.572	3.7	6.01	52	6.75	64	61	655–56	*		*	*	*
D	7.512	1.2	7.47	80	8.13	94	81	750–51	*	*	*		*
E	9.640	2.1	9.1	125	9.95	136	132	963–64	*				
F	10.465	5.2	10.34	148	10.56	156	152	1045–46	*		*	*	
G	11.378	5.8	11.04	166	11.4	176	175	1134–35	*		*	*	
H	12.025	2.5	11.72	194	13.47	214	197	1201–202	*		*	*	
I	13.266	0.8	11.72	194	13.47	214	212	1326–327	*		*	*	*
J	14.889	4.3	14.19	234	14.93	250	249	1487–488	*		*		
KA	16.410	1.0	15.89	266	16.63	288	282	1640–641	*		*		
KB	16.480	3.0	15.89	266	16.63	288	283	1647–648	*		*		*
L	17.242	2.8	17.05	296	17.78	316	301	1722–723	*		*		*
M	17.430	7.4	17.05	296	17.78	316	305	1742–743	*		*		*
N	18.624	2.5	18.38	328	18.96	342	334	1860–861	*				*
O	19.360	3.8	19.24	348	19.74	358	350	1935–936	*		*	*	*
P	21.450	5.0	21.26	392	22.21	420	396	2143–144	*		*		
Q	22.330	4.0	22.21	420	22.56	434	424	2232–233	*		*		*
R	24.042	1.2	22.84	452	24.25	482	478	2403–404	*				*
S	34.720	1.0	34.65	808	34.73	820	818	3471–472	*		*		*
T	35.640	1.0	35.61	858	35.91	870	859	3563–564	*				*
U	35.910	2.0	35.61	858	35.91	870	870	3590–591	*				*

[a] The depth-age control points at Core MD97-2142, available from *Wei et al.* [2003], were recognized by the correlation of the profile of oxygen isotope data of this core with the low-latitude stack.
[b] Asterisks mark the minerals that were recognized in each tephra layer.
[c] Average value plus and minus 1 SD.
[d] Average value plus and minus 2σ.
[e] Types I–V: Please refer to the text or Figures 6 and 7.
[f] Source area: SWM, southwestern part of Macolod Corridor; MM, middle section of Macolod Corridor; NEM, northeastern part of Macolod Corridor; BS, Bataan Segment [*Ku et al.*, 2008]; and UC, uncertain in this paper.
[g] The depth–astronomical ages of Core MD97-2143 were recognized by the astronomic calibration method [*Horng et al.*, 2002].

(n = 150) for $^{87}Sr/^{86}Sr$. All analyses were performed at the Academia Sinica in Taiwan.

4. Results

4.1. Occurrence and Age of the Tephra Layers

[17] Both Cores MD97-2142 and MD97-2143 record long periods during which no discrete tephra layers were deposited. The tephra layers in both cores are described in Table 1, which also includes data on the stratigraphic depths, layer thicknesses, and calculated ages. In Core MD97-2142, 22 tephra layers (designated layer A to layer U) can be identified over the past 870 ka Three layers occur between 870 and 818 ka, followed by a long gap from 818 to 478 ka, and the remaining 19 tephra layers are densely clustered after 478 ka. The youngest tephra layer recorded in Core MD97-2142 is at 6 ka.

[18] In Core MD97-2143 (Table 1), ten tephra layers (designated layers 1 to 10) are recognized over the past 1977 ka. These ten layers show a gap (a period of relative volcanic quiescence) between 301 and 1355 ka, with four of the layers having ages younger than 301 ka and the other six layers are older than 1355 ka. The youngest tephra layer recorded in Core MD97-2143 is 172 ka.

4.2. Glass Particles and Tephra Layers

[19] The tephra layers consist predominantly of vesicular glass particles and subsidiary volcanic minerals such as plagioclase, clinopyroxene, orthopyroxene, biotite amphibole and quartz (Figure 5 and Table 1; identified from EMPA). The freshness of the glass particles is supported by the clear glass surface and the well-preserved vesicular texture. The glass particles in 25 of the layers range in color from brown to light brown; only in seven of the layers are they colorless in color. The major element geochemistry of glass particles with a total oxide value of greater than 95 wt % might attest to the glass particles' freshness. In addition, the range in $^{87}Sr/^{86}Sr$ observed coincides well with the range of ratios observed for the volcanics sampled onshore (Figures 3 and 6). The $^{87}Sr/^{86}Sr$ value and Sr concentration in the modern ocean are 0.709 and up to one thousand ppm, respectively. Therefore, if the glass particles were altered by seawater, even to a minor degree, the $^{87}Sr/^{86}Sr$ ratio of the glass particles would have obviously increased and exhibited a range of compositions shifted toward higher values relative to values observed for the volcanics sampled onshore. However, Figure 6 shows that the $^{87}Sr/^{86}Sr$ values of glass particles are around 0.704–0.705 with very little variation, which strongly suggests that these glasses have not been significantly exchanged Sr with seawater.

[20] On the basis of the major element geochemistry of the glass particles, the tephra layers can be classified into five types (Tables 1 and 2). Figure 7 shows three types in Core MD97-2142 (types I–III) and four in Core MD97-2143 (types I, III, IV and V). The variation in $^{87}Sr/^{86}Sr$ values for the glass particles in the two cores, ranging between 0.70384 and 0.70530 (Table 2), shows no clear relationship to the stratigraphic depth (Figure 6) at which the glass particles accumulated, but instead appears to depend on the type of tephra layer. The geochemical characteristics of each type and the chronologies of each type are described below.

4.2.1. Core MD97-2142

4.2.1.1. Type I Tephra Layers

[21] The 16 type I tephra layers (layers A–C, layers E–KA and layers M–R) contain glass particles with 55.9–71.5 wt % SiO_2 and 1.1–3.6 wt % K_2O, and cluster tightly along the boundary between the calc-alkaline series and the high-K series (Figure 7). The $^{87}Sr/^{86}Sr$ ratios of the glass particles range from 0.70460 to 0.70530 (Figure 6). The tephras were deposited after 478 ka (Table 1 and Figure 6) and have an average repose time of around 31 ± 15 (1 SD) ka. The youngest tephra layer recorded was deposited at around 6 ka.

4.2.1.2. Type II Tephra Layers

[22] Two layers are classified as type II tephra layers: layers KB and L (Table 1 and Figure 7). The glass particles in these tephras, characterized by 57.2–63.2 wt % SiO_2 and 3.2–5.1 wt % K_2O, fall into the field of the shoshonitic series in the Harker diagram (Figure 7). The $^{87}Sr/^{86}Sr$ ratios for the glass particles range from 0.70406 to 0.70414 (Figure 6). The tephra layers are dated at 283 ka (KB) and 301 ka (L).

4.2.1.3. Type III Tephra Layers

[23] The type III tephra layers include the four tephra layers D, S, T, and U (Table 1 and Figure 7). Their glass particles are characterized by 72.6–79.3 wt % SiO_2 and 2.1–5.2 wt % K_2O, and are

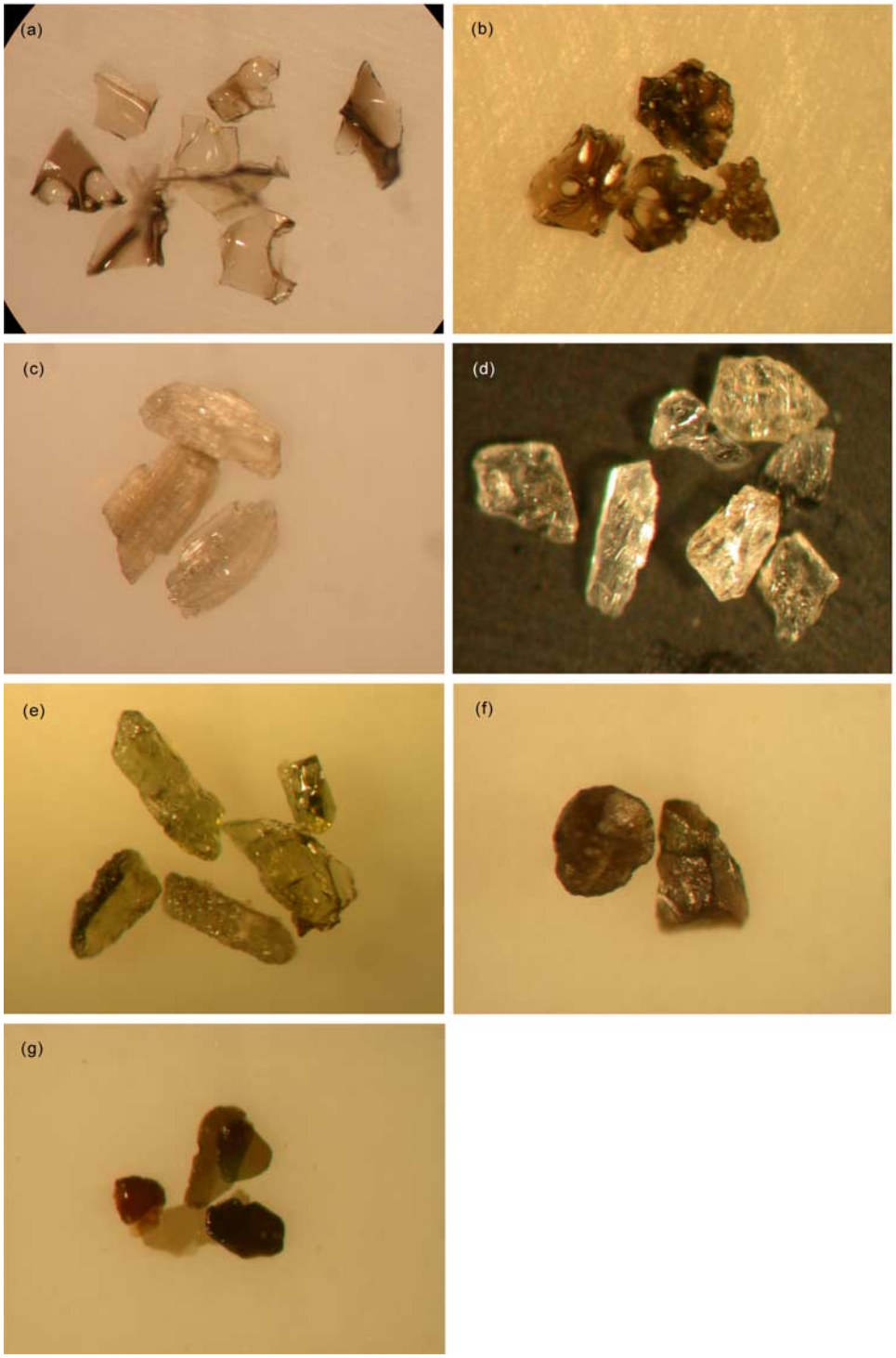

Figure 5. Images of (a–c) glass particles and (d–g) minerals under a microscope. Grain size is in the range of 125–250 μm. Figure 5a shows disk-like glass particles with spherical vesicles, Figure 5b shows irregular glass particles with spherical vesicles, Figure 5c shows rod-like glass particles with elongated vesicles, Figure 5d shows plagioclase, Figure 5e shows clinopyroxene, Figure 5f shows orthopyroxene, and Figure 5g shows biotite.

grouped in the calc-alkaline series and high-K series in the Harker diagram (Figure 7). Glass particles in the tephra layers S and U fall into two compositional groups, low-K glasses and high-K glasses (Figure 7); these are recognized in the different particles of these layers. The $^{87}Sr/^{86}Sr$ ratios for type III glass particles are 0.70399–0.70443 (Figure 6). These tephras accumulated at

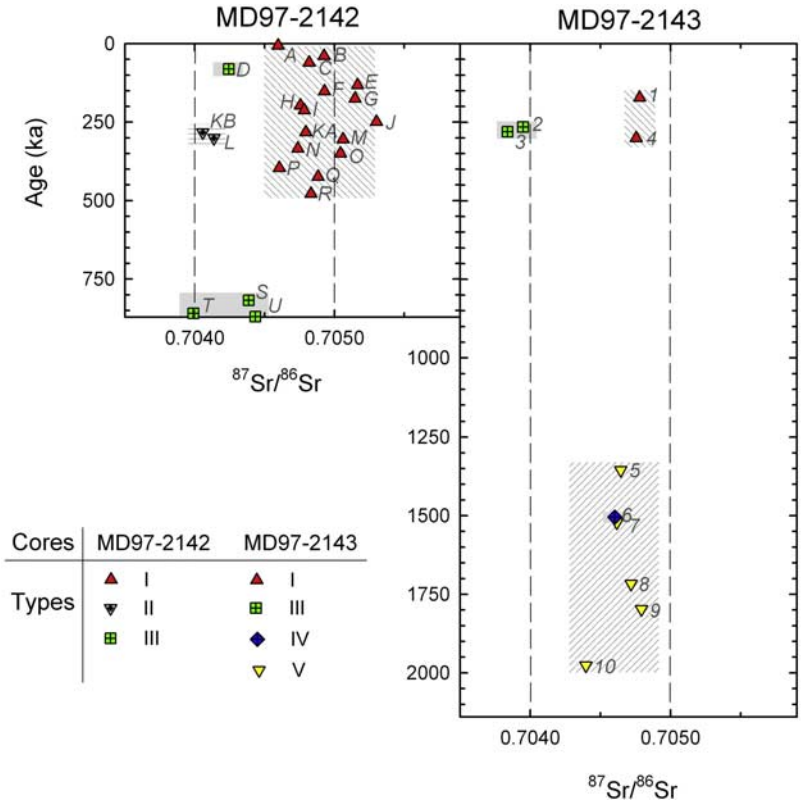

Figure 6. Sr isotope ratios of tephra layers A–U and 1–10 and their classification into types I–V as discussed in the text (section 4.2) and as shown in Figure 7. The shadowed areas mark the accumulation period for each type of tephra layer.

ages 81 ka (layer D) and 818–870 ka (layers S, T, and U).

4.2.2. Core MD97-2143

4.2.2.1. Type I Tephra Layers

[24] The geochemistry of the glass particles from the type I tephra layers in Core MD97-2143 (layers 1 and 4) is similar to that of the type I tephra layers in Core MD97-2142, though their range in SiO_2 (55.1–67.3 wt %) is more restricted. The type I tephra layers 1 and 4 in Core MD97-2143 (ages 172 ka and 301 ka, respectively) were erupted in the same period as the type I tephra layers in Core MD97-2142 (<478 ka) (Table 1 and Figure 6). The Sr isotopic ratios of the glass particles fall between 0.70476 and 0.70478 (Figure 6), which is at the lower end of the range observed for type I glasses in Core MD97-2142.

4.2.2.2. Type III Tephra Layers

[25] The glass particles of the type III tephra layers (layers 2 and 3) have a high silica content (77.8–79.2 wt %) (Figure 7) and overlap in composition with the low-K glasses of the type III tephra layers in Core MD97-2142. The Sr isotopic ratios of the glass particles of the type III layer in Core MD97-2143, 0.70384–0.70395, are also similar to those of the type III layer in Core MD97-2142 (Figure 6). The depositional ages of the type III tephra layers in Core MD97-2143 (2 and 3) are 266 and 281 ka (Table 1 and Figure 6), respectively, and these are also within the age range of the type III layer of Core MD97-2142.

4.2.2.3. Type IV Tephra Layers

[26] The glass particles of the type IV tephra layer (layer 6) have a high silica content (77.6–80.2 wt %; Figure 7). The glass particles of types IV and III, 2.0–2.9 wt % K_2O, are indistinguishable from one another in the Harker diagram (Figure 7). However, the Sr isotopic ratio of the glass particles of the type IV layer, 0.70460, is higher than that of the type III layer, which ranges from 0.70384 to 0.70395 (Figure 6). The depositional age of the type IV tephra layer is 1505 ka (Table 1 and Figure 6).

4.2.2.4. Type V Tephra Layers

[27] The glass particles of the five type V tephra layers (layers 5, 7, 8, 9, and 10) are characterized by 56.0–67.7 wt % SiO_2 and 2.0–5.0 wt % K_2O. The glass particles of the type V tephra layers belong to

Table 2 (Sample). Results of Chemical Analyses of the Glass Particles in the Two Deep-Sea Cores MD97-2142 and MD97-2143[a] [The full Table 2 is available in the HTML version of this article]

	Layers															
	A		B		C		D		E		F1		F2		G3	
Major Oxides	Mean (wt %)	1s	Mean (wt %)	1s	Mean (wt %)	1s	Mean (wt %)	1s	Mean (wt %)	1s	Mean (wt %)	1s	Mean (wt %)	1s	Mean (wt %)	1s
SiO_2	59.14	0.98	58.38	0.95	66.00	1.17	77.30	1.47	58.11	1.55	69.24	1.13	66.52	5.06	69.85	0.71
TiO_2	0.86	0.08	1.00	0.10	0.76	0.08	0.10	0.05	0.91	0.05	0.60	0.08	0.69	0.20	0.60	0.07
Al_2O_3	16.13	0.36	16.04	0.30	15.02	0.43	13.58	1.10	16.29	0.29	15.20	0.34	15.21	0.48	14.83	0.32
FeO	8.76	0.37	8.70	0.34	5.91	0.49	0.56	0.18	8.71	0.70	4.37	0.45	5.71	2.20	4.52	0.21
MnO	0.18	0.05	0.15	0.07	0.15	0.05	0.03	0.02	0.18	0.05	0.13	0.03	0.13	0.05	0.14	0.05
MgO	3.07	0.25	3.41	0.27	1.45	0.32	0.14	0.06	3.15	0.37	0.70	0.15	1.40	1.19	0.87	0.09
CaO	6.50	0.47	7.14	0.28	3.88	0.53	1.23	0.39	6.96	0.77	2.49	0.32	3.68	1.98	2.71	0.22
Na_2O	3.51	0.10	3.32	0.26	4.06	0.24	4.16	0.32	4.07	0.22	4.12	0.47	3.90	0.49	3.64	0.65
K_2O	1.86	0.13	1.86	0.13	2.77	0.33	2.91	0.36	1.63	0.22	3.15	0.16	2.77	0.80	2.84	0.10
	n = 24		n = 11		n = 25		n = 8		n = 9		n = 36		n = 48		n = 15	

	Layers															
	A		B		C		D		E		F1		F2		G3	
	Mean	2σ	Mean	2σ	Mean	2σ	Mean	2σ	Mean	2σ	Mean	2σ	Mean	2σ	Mean	2σ
$^{87}Sr/^{86}Sr$	0.704600	0.00002	0.70493	0.00004	0.70482	0.00005	0.70424	0.00002	0.70517	0.00003	0.70493	0.00002	n.a.		0.70515	0.00003

[a] n.a., not analyzed; s or σ, standard deviation. For F1, F2, G3 and G4 please refer to Table 1.

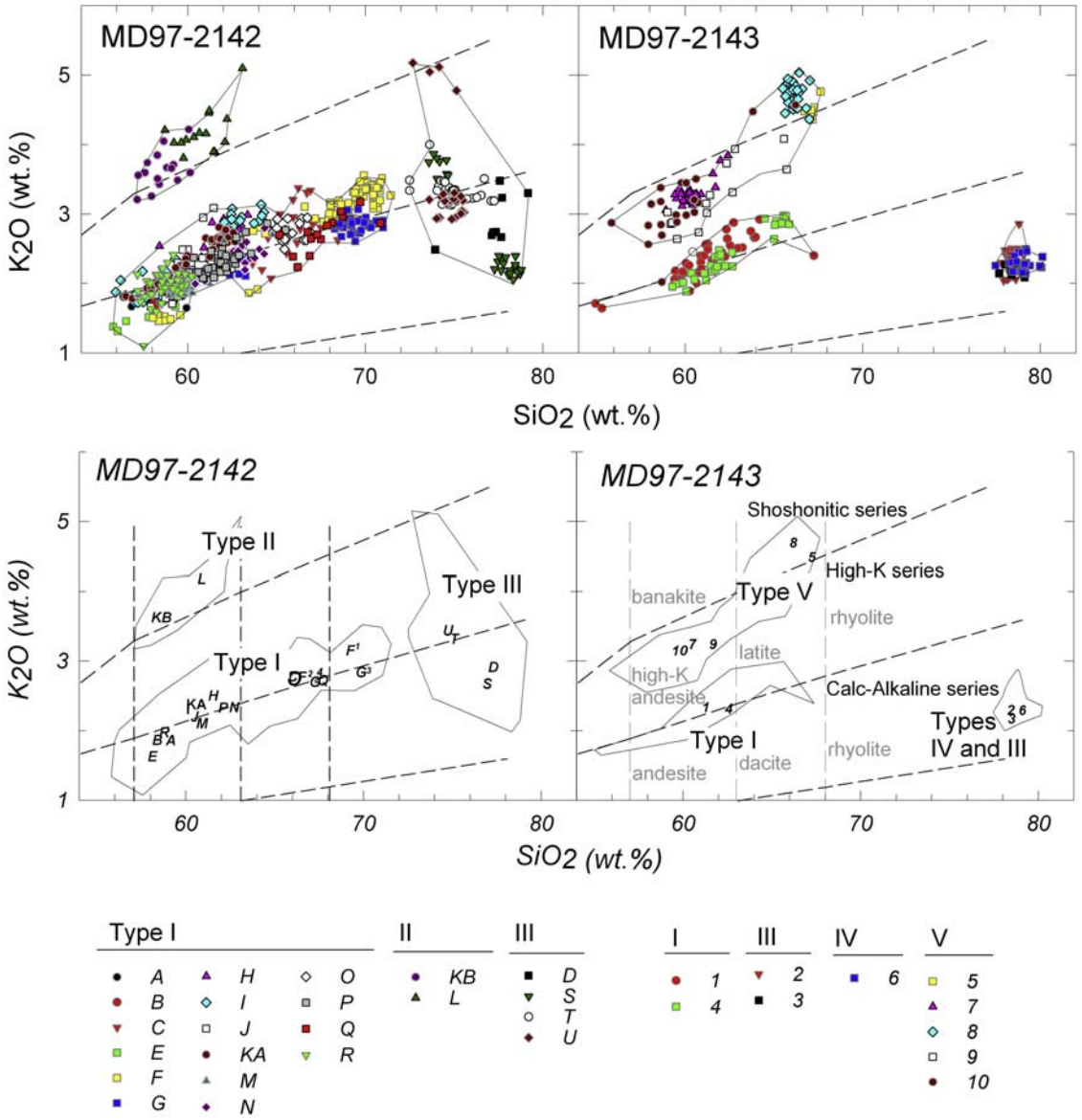

Figure 7. Classification of the tephra layers A–U and 1–10 into five types (I–V) based on glass particle K_2O and SiO_2 contents. Solid lines demarcate the data distribution for each type of tephra layer. (top) The data are displayed using raw data for each layer. (bottom) The data are displayed using the mean value for each layer, marked by the appropriate nomenclature. The nomenclatures for volcanic rocks and rock series follow those of *Rickwood* [1989].

the high-K series and the shoshonitic series (Figure 7). The $^{87}Sr/^{86}Sr$ ratios of these glass particles range from 0.70440 to 0.70479 (Figure 6). The type V tephra layers were all deposited between 1355 and 1977 ka (Table 1 and Figure 6), and have average repose times of around 156 ± 52 (1 SD) ka.

5. Discussion

5.1. Tephra Sources

[28] In explosive eruptions, magma is fragmented by the rapid exsolution of dissolved volatile components to produce pyroclastic materials. The fine-grained portions of these materials (tephra) are distributed over a wide area far from the source volcano according to the dominant wind direction above the volcano at time of eruption, hence tephra of different eruptions of a single volcano may be dispersed in different directions. Magma is usually composed of silicate melt and crystallized minerals (phenocrysts) suspended in the melt; thus, tephra consists of glass particles and minerals. The glass is quenched melt that may have a more evolved composition than the magma (melt + phenocrysts). Many petrological and geochemical studies of

volcanoes all over the world have revealed that the chemical compositions of magma can be distinguished among volcanoes. This has been used to classify regional magma types, and thus to distinguish volcanoes from one another. Tephra are known to correspond compositionally to the magma from a source volcano, and vice versa, analysis of the glass particles in tephras can provide information on magma from the source volcano [*Nakagawa and Ohba*, 2002]. To study each explosive event at a source volcano, detailed investigations of the geochemistry of glasses and minerals for both onland (proximal) samples and deep-sea (distal) tephras will be needed. Preliminary of this work for Mount Pinatubo in the Luzon Island has already been completed by *Ku et al.* [2008].

[29] In conjunction with existing geochemical and chronological data for onshore Quaternary volcanic rocks, the geochemical characteristics and estimated accumulation ages of the tephra layers reported in this study can be used to infer tephra sources. Distinct source areas may be identified for type I and V tephras, and nonspecific source areas can be identified for type II–IV tephras, as discussed below.

[30] 1. The bulk of type I tephra layers is traceable to the southwestern and middle sections of the Macolod Corridor, with layer B also traceable to the northeastern corridor. The geochemical compositions of the glass particles in type I tephras (Figures 6 and 7) are similar to the geochemical compositions of the onshore Quaternary volcanic rocks of the southwestern and middle sections of the Macolod Corridor, which contain 47.4–69.6 wt % SiO_2, 0.4–3.5 wt % K_2O, and $^{87}Sr/^{86}Sr$ ratios of 0.7041–0.7059 [e.g., *Oles*, 1991; *Knittel and Oles*, 1995] (Figures 2 and 3).

[31] Layers E, G, and J of type I are characterized by 55.9–71.1 wt % SiO_2, 1.3–3.1 wt % K_2O, and Sr isotopic ratios > 0.7051, and are thus also geochemically similar to the volcanic rocks of the western belt of the Mindoro Segment, which contain 55.9–60.0 wt % SiO_2, 1.8–3.0 wt % K_2O and a 0.7051–0.7054 $^{87}Sr/^{86}Sr$ ratio [*Knittel and Defant*, 1988; *Defant et al.*, 1991]. However, on the basis of the available K-Ar data reported for the volcanic rocks of this belt, i.e., 0.82 Ma, 1.56 Ma, and 1.64 Ma [*de Boer et al.*, 1980], this region can perhaps be discounted as a possible source for layers E, G, and J (132–249 ka). Alternatively, the presence of these layers could indicate that volcanism in the Mindoro segment continued much longer than is indicated by the currently very sparse age data.

[32] The geochemical compositions of the glass particles in some type I layers (A, B, E, H, J, KA, M, N, P and R) are also similar to the geochemical compositions of the onshore Quaternary volcanic rocks in the northeastern part of the Macolod Corridor, which contain a wide range of K_2O content at 53–66 wt % SiO_2 and $^{87}Sr/^{86}Sr$ ratios of 0.7040–0.7051 [e.g., *Oles*, 1991; *Knittel and Oles*, 1995] (Figures 2 and 3). However, on the basis of the available age data for the volcanic rocks of the northeastern part (Figure 4), the Laguna de Bay Caldera, where the last eruption occurred after 50 ka [*Vogel et al.*, 2006], and Mount Banahaw, with its Holocene eruptions, are possible sources only for the two youngest tephra layers, layers A and B (6 and 39 ka, Table 1). For the other type I tephra layers, deposited in the age range of 61 to 478 ka, no corresponding ages are known in the onshore record in the northeastern part of corridor.

[33] The accumulation ages for the type I tephra layers, all younger than 478 ka, coincide with the ages of the volcanic products associated with large explosive eruptions in the middle and southwestern sections of the Macolod Corridor. Ages for onshore volcanics in the middle and southwestern sections (Figure 4) include (1) Mount Makiling (middle section), 0.01–0.51 Ma by K-Ar dating [*de Boer et al.*, 1980; *Wolfe*, 1981; *Defant et al.*, 1991; *Sudo et al.*, 2000]; (2) Taal Tuff (southwestern section), not older than 0.3 ± 0.18 Ma by stratigraphic superposition [*Sudo et al.*, 2000]; (3) older ignimbrites of Taal Lake Caldera (southwestern corridor), 100–500 ka by K-Ar and Ar-Ar dating [*Torres et al.*, 1995]; and (4) caldera-genetic pyroclastic flows for Taal Lake Caldera (southwestern corridor), 5.4–140 ka or 5.4–27 ka by ^{14}C dating and stratigraphic superposition [*Listanco*, 1994]. Moreover, the most recent occurrence of type I tephra layers (layer A), recorded at 6 ka in Core MD97-2142 (Table 1), is in accordance with the age of the pyroclastic flow from the youngest caldera-forming eruption of the Taal Lake Caldera, ^{14}C-dated at 5380 ± 70 or 5670 ± 80 B.P. [*Listanco*, 1994; *Torres et al.*, 1995]. The volume of this pyroclastic flow has been estimated at up to 50 km^3 [*Listanco*, 1994]. The silica content of this flow [*Listanco*, 1994] is slightly lower than that of the glass particles deposited in the 6 ka layer (layer A) of Core MD97-2142 (Figure 8), but glasses are typically more silica-rich than whole

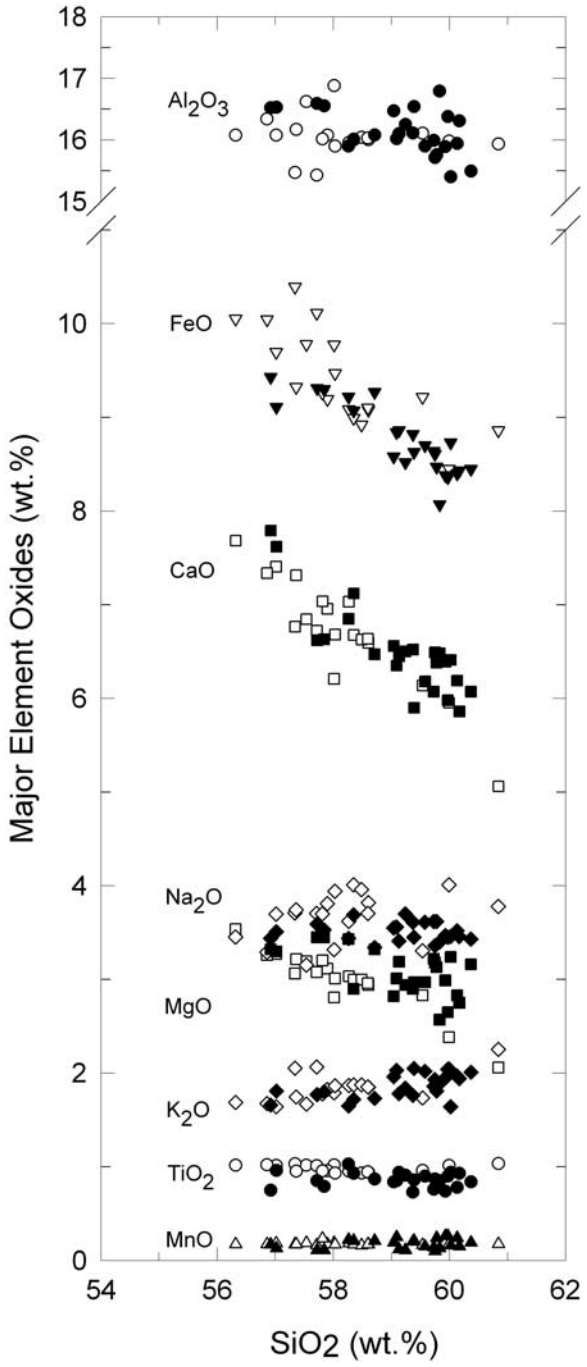

Figure 8. Harker diagram for the glass particles in tephra layer A (6 ka) and for the volcanic rocks of the last caldera-forming eruption of Taal Lake. Solid symbols indicate glass particles; open symbols indicate volcanic rocks. Volcanic rock data are from *Listanco* [1994].

rock samples which represent mixtures of minerals and matrix glass [*Pouclet et al.*, 1991].

[34] 2. Type V tephra layers are traceable to the northeastern Macolod Corridor. Type V tephra layers, comprising five layers in Core MD97-2143, are considered to have been sourced from the northeastern Macolod Corridor. Glass particle compositions of type V tephras (Figures 6 and 7) overlap with those recorded for volcanic rocks from the northeastern section of the corridor. The Quaternary volcanic rocks from the northeastern section typically contain 50.9–66.0 wt % SiO_2, 0.7–6.7 wt % K_2O, and 0.7040–0.7051 for $^{87}Sr/^{86}Sr$ [*Defant and Ragland*, 1988; *Knittel and Defant*, 1988; *Mukasa et al.*, 1994] (Figures 2 and 3).

[35] The available K-Ar chronologies for the lava, tuff, and ignimbrite from the northeastern section of the corridor span from 1.0 to 2.24 Ma (1.0–1.1 Ma, n = 4, and 1.67–2.24 Ma, n = 6 for Laguna de Bay; 1.02–1.71 Ma, n = 9 for Mount San Cristobal; 1.29–1.53 Ma, n = 3 for Mount Banahaw) [*de Boer et al.*, 1980; *Sudo et al.*, 2000] (Figure 4). These ages coincide with the accumulation period for the type V tephra layers, which ranges from 1355 to 1977 ka (Figures 6 and 9). However, the youngest calderagenic events for the Laguna de Bay Caldera recorded from onshore investigations of a tuff formation (5 ka, 27–29 ka, and >42 ka by ^{14}C dating) by *Catane et al.* [2004, 2005] could correspond to layer B of the type I tephra layers, as discussed above.

[36] 3. Type II, III and IV tephra layers are traceable to nonspecific sources on Luzon Island. Type II tephra layers could not be clearly identified in the products released from the Macolod Corridor because of their high K_2O contents (3.2–5.1 wt % K_2O at 57.2–63.2 wt % SiO_2). The $^{87}Sr/^{86}Sr$ ratios (0.70406–0.70414) of the glass particles (Figures 6 and 7) are also lower than those of volcanic rocks in the Macolod Corridor (Figures 2 and 3).

[37] Likewise, the seven tephra layers of types III and IV, with glass particle silica contents in excess of 72.6 wt % (Figure 2), could not be satisfactorily correlated with the rhyolites of the Macolod Corridor. Available data for rhyolites in the corridor are scarce, limited to two rhyolite tuff layers found at Mount Makiling [*Vogel et al.*, 2006] and an altered rhyolitic tuff layer from the Laguna de Bay area [*Oles*, 1991]. The reported ages for the rhyolites are 350 ka and 500 ka for Mount Makiling, by U/Pb zircon SHRIMP dating [*Vogel et al.*, 2006], and 1.10 ± 0.06 Ma by K-Ar dating for the rhyolites from the Laguna de Bay area [*Oles*, 1991] (Figure 4). However, these ages offer no exact match for the estimated ages of the tephra layers accumulated at 81 ka (layer D, type III layer), 266–281 ka (layers 2 and 3, type III layers),

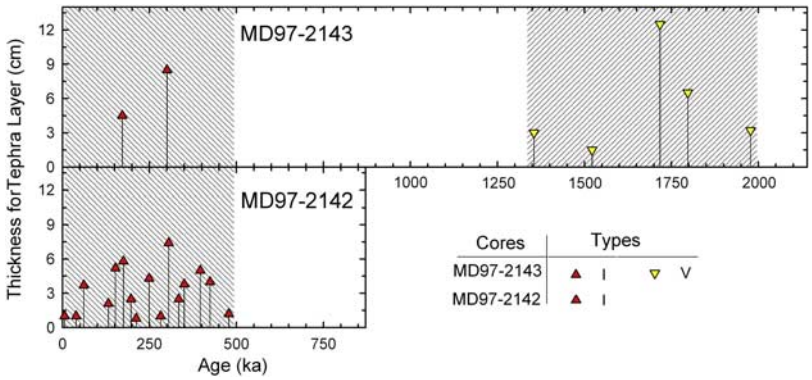

Figure 9. Diagram of thickness versus deposition age for each tephra layer that is traceable to large, explosive eruptions in the Macolod Corridor. The shadowed areas mark the accumulation period for each type of tephra layer. Tephrostratigraphies from the two cores record two active periods in which tephra layers occur frequently and a quiet period that lacks records of discrete tephra layers.

818–870 ka (layers S-U, type III layers) and 1,505 ka (type IV layers), respectively (Figure 6).

[38] On the basis of Sr isotopic ratios of the glass particles, these tephras could be products released from explosive eruptions in several volcanic provinces on Luzon Island (Figure 3), except for the Mindoro Segment. The glass particle Sr isotopic ratios, ranging between 0.7038 and 0.7046, differ from those of the Mindoro Segment, which are generally above 0.7051 [*Defant et al.*, 1991; *Knittel and Defant*, 1988]. The glass particle Sr isotopic ratios of the type III and IV tephras, 0.7040–0.7044 and 0.7046, respectively, overlap with the ratios of the volcanic rocks from both the Bataan Segment [e.g., *Defant et al.*, 1991; *Castillo and Punongbayan*, 1996] and the Macolod Corridor [e.g., *Defant and Ragland*, 1988; *Oles*, 1991]. layers T, 2 and 3 of the type III layers, with Sr isotopic ratios of 0.7040, 0.7039 and 0.7038, respectively, overlap with the ratios of the volcanic rocks from the North Luzon Segment [e.g., *Defant et al.*, 1990; *McDermott et al.*, 1993], the Bataan Segment [e.g., *Defant et al.*, 1991; *Castillo and Punongbayan*, 1996], and the Bicol Arc [e.g., *McDermott et al.*, 2005; *DuFrane et al.*, 2006]. Therefore, the seven tephra layers containing glass particles with rhyolitic compositions can be associated with the North Luzon Segment, the Bataan Segment, the Macolod Corridor and/or the Bicol Arc.

5.2. Quaternary Volcanic Eruptions in the Macolod Corridor

5.2.1. Large Explosive Eruptions

[39] The bulk (23 out of 32) of the tephra layers with glass particle silica contents of <71.5 wt % provide a record that can constrain the history of large, explosive eruptions in the Macolod Corridor over the past 2 Ma, including the active eruption periods, eruption areas, and repose times (Figure 9). The record is constrained by two deep-sea cores that cover the past 870 ka for Core MD97-2142, and 2140 ka for Core MD97-2143. The 23 tephra layers belong to the two periods of older than 1355 ka and younger than 478 ka. The eruptions primarily occurred in these two periods, which were separated by a relatively quiet period lasting from 1355 to 478 ka. In addition, the locus for the older large explosive eruptions was in the northeastern section of the corridor, and thereafter shifted to the middle and southwestern sections. Toward the end (<50 ka) of the younger period, however, the northeastern section may have been volcanically active again.

[40] Core MD97-2143 records five large explosive events in the northeastern section of the corridor for the first active period (1355–1977 ka), and two events in the middle and southwestern sections for the second period (478–0 ka). Core MD97-2142 also indicates a relatively quiet period (478–870 ka) after which the middle and southwestern sections of the corridor became the dominant active areas with 16 explosive events recorded (type I tephra layers in Core MD97-2142). However, the northeastern part of the corridor could not be discounted as a possible source for tephra layer B.

[41] For the 16 large explosive eruptions in the Macolod Corridor recorded in Core MD97-2142 of the second active period (478–0 ka), the repose time was 31 ± 15 ka. The last event occurred at 6 ka, for which the eruption volume has been estimated as up to 50 km^3 in volume [*Listanco*, 1994]. For Core MD97-2143, the tephras were

deposited less frequently. In the first active period (1355–1977 ka), five tephra layers are recorded, on average one every 156 ± 52 ka (Figure 9). This time interval is similar to the repose interval of 129 ka between the two large explosive events (layers 1 and 4) recorded in the second active period 0–478 ka. The last event recorded in Core MD97-2143 was at 172 ka.

[42] The difference in the number of tephra layers from the two cores, 16 layers in Core MD97-2142 and 2 layers in Core MD97-2143, may have resulted from the prevailing winds (easterlies) above this region, if the assumed wind directions in the past 2 Ma are similar to those in the modern era (modern wind data are available at http://data.ecmwf.int/data/). On the basis of this assumption, tephras released from the general eruption on this region would be easily transported to the west (site MD97-2142) because of the easterly winds. Only exceptional eruptions could disperse tephras to the east (site MD97-2143). Exceptional eruptions include either a powerful volcanic plume with sufficient internal energy to force the tephras to the east against prevailing easterlies, or a certain plume column height in an opportune season that could transport tephras to the east by an alternate wind system (westerlies). Following this assumption, prevailing easterlies and less powerful eruptions in the southwestern Macolod Corridor may have been the reason that volcanism in the southwestern corridor is not recorded in the stratigraphy of 1355–1977 ka in Core MD97-2143.

5.2.2. Explosive and Effusive Eruptions

[43] As discussed in the foregoing sections (sections 5.1 and 5.2.1), the available age data for volcanic rocks in stratovolcanoes and calderas in the Macolod Corridor (Figure 1) are in broad agreement with the ages of the tephras in the two identified volcanically active periods (478–0 ka and 1977–1355 ka). It is important to note, however, that ages for the monogenetic volcanoes in the middle section of the Macolod Corridor (Figure 1) coincide with the relatively quiet period (1355–478 ka) recorded in the tephrostratigraphies. These monogenetic volcanoes, composed of small scoria cones and lava domes, exhibit K-Ar ages mostly younger than 1 Ma (Figure 4) [*de Boer et al.*, 1980; *Oles*, 1991; *Sudo et al.*, 2000]. The 1 Ma datum for the beginning of monogenetic volcanism loosely coincides with the starting age of the relatively quiet period based on tephrostratigraphy. In this relatively quiet period, the stratovolcanoes (Mounts Malepunyo, Banahaw and San Cristobal) were also active (Figure 4), but these activities could not be recorded in these two deep-sea sites, perhaps because of their relatively smaller eruption magnitudes. The tephrostratigraphies (Figure 9) recorded this relatively quiet period as being terminated by a series of large explosive eruptions occurring in the southwestern Macolod Corridor and in the middle section of the corridor after 478 ka.

[44] Therefore, the Quaternary Macolod Corridor volcanic events can be divided into three periods: the older (1977–1355 ka), middle (1000–478ka or 1355–478 ka), and younger (478–0 ka) periods (Figures 10a–10c). In the older period, the active volcanic area likely aligned itself along two lines in the southwestern and northeastern sections of the corridor (Figures 4 and 10a). This configuration of two lines of volcanoes was reported by *Oles* [1991]. The volcanoes in the northeastern section produced large explosive eruptions occurring, every 156 ± 52 ka on average, as recorded at site MD97–2143 in the Philippine Sea basin.

[45] In the middle period (Figure 10b), the active volcanic area migrated southwestward to the middle section and the southwestern part of the corridor. In this period, instead of large explosive eruptions identifiable in the deep-sea stratigraphy, relatively smaller explosive eruptions of the stratovolcanoes were active and numerous small monogenetic explosive and effusive eruptions took place and formed small scoria cones and lava domes along the corridor.

[46] The active volcanic area for large explosive eruptions in the younger period appears to have continued its southwestward migration to the Taal Lake Caldera, which has been reported to possess four caldera-forming eruptions with ages <140 ka [*Listanco*, 1994]. The younger period was characterized by large explosive eruptions that occurred on average every 31 ± 15 ka. During the younger period (Figure 10c), the monogenetic and polygenetic volcanism initiated in the middle period remained active in the middle section of the corridor. In the most recent part of this younger period, volcanism in the northeastern part of the corridor was again active (Figure 4).

5.3. Evolution of the Subducted Slab and Active Quaternary Volcanoes

[47] Using the new chronological constraints provided by the deep-sea tephra record in combination with age and geochemical data from on-land volcanoes, the evolution of the subducted slab under-

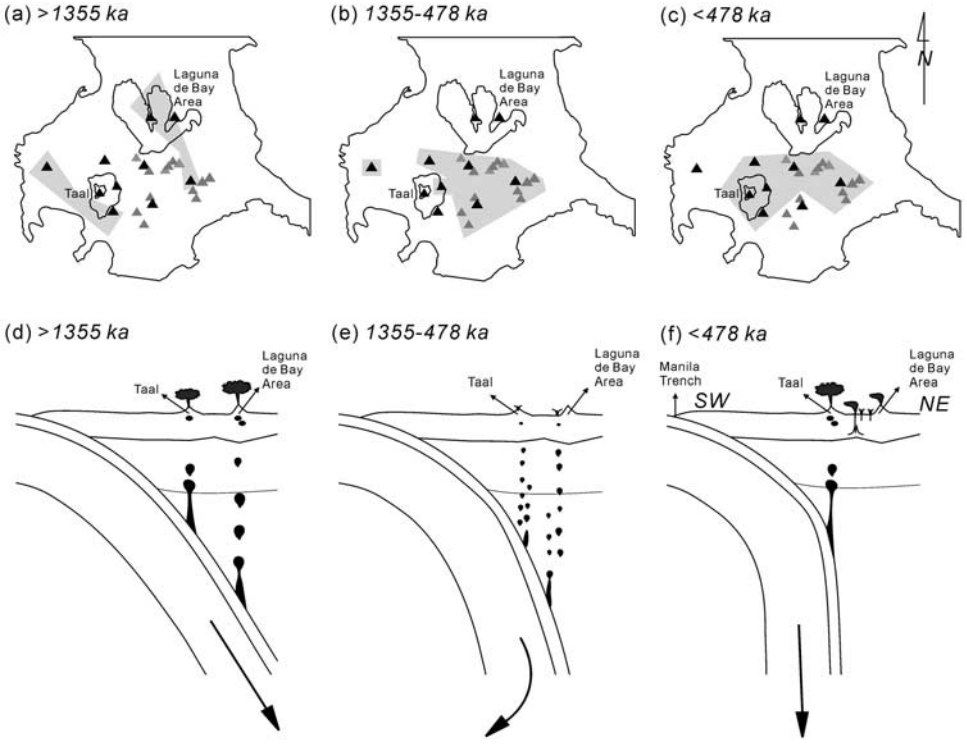

Figure 10. (a–c) Maps illustration the migration of the volcanic activity in the Macolod Corridor during the Quaternary and (d–e) cartoons illustrating the corresponding evolution of the subducted slab under the Macolod Corridor. The black triangles denote Quaternary volcanoes, gray triangles denote Quaternary monogenetic volcanoes, and shaded gray areas denote active volcanic areas with respect to each specific period.

neath the Macolod Corridor and of the active Quaternary volcanoes can be interpreted in terms of three distinct periods (Figures 10d–10f). During the older period (>1355 ka), the subducted slab underlying the corridor probably experienced relatively stable conditions in terms of its dip angle and subduction rate. Under such stable conditions, the dehydration of the slab and melting at two specific depths [*Tatsumi and Eggins*, 1995] could have contributed to the formation of magma from the mantle wedge that fed the volcanoes lying along two lines across the corridor (Figures 4, 10a, and 10d). The volcanoes on the northeastern line released magmas with higher potassium content than those on the southwestern line. The difference in the potassium content of the two lines of volcanoes might be explained by the potassium-depth (K-h) relationship that has been globally recognized for arc systems [*Dickinson*, 1975; *Tatsumi and Eggins*, 1995]. Moreover, because of a regular supply of magma under such stable conditions [*Huang and Lundstrom*, 2007], if the volume of magma stored over the long-term storage in the chamber was sufficient, it could have been released to the surface by regular (frequent) large explosive eruptions over a long period of time [*Denlinger and Hoblitt*, 1999; *Jellinek and DePaolo*, 2003; *Scandone et al.*, 2007]. Each large explosive eruption could have released large amounts of tephra deposited simultaneously on land and in the surrounding deep-sea basins.

[48] In the middle period, 1355 to 478 ka, the morphology of the subducted slab steepened beneath the corridor (Figure 10e). The locus of active volcanism on the northeastern line migrated southwestward to the middle section of the corridor (Figure 10b) and no longer stayed above the subducted slab (Figure 10e), whereas the locus of active volcanism on the southwestern line migrated only slightly from Mount Macolod to Mount Sungay in the southwestern section (Figure 10b) and remained above the subducted slab supplying magma (Figure 10e). The possible starting age for this slab adjustment is constrained between the ages of the last occurrence of the large explosive eruptions (1355 ka) in the northeastern section of the corridor and the oldest monogenetic volcanism (dated at 1 Ma) in the middle section (Figure 4). Under such conditions of slab steepening, magma

with MORB signatures could be produced by decompression melting of the mantle wedge [*Kincaid and Griffiths*, 2004]. Moreover, because of a more irregular and unstable supply of magma into the chamber during the dynamic instability caused by slab steepening, there may have been a lower volume of stored magma, and it could have been released to the surface by small monogenetic explosive and effusive eruptions as well as by small polygenetic eruptions [*Barmin et al.*, 2002].

[49] During the younger period, since 478 ka, the morphology of the subducted slab underlying the corridor again experienced relatively stable conditions as in the older period (<1355 ka), but with a steeper dip angle (Figure 10f). The volcanoes in the southwestern section of the corridor (Taal Lake Area) still lie above the subducted slab supplying melt and/or fluid into the mantle wedge, and erupt magmas that possess the geochemical signals of a typical island arc. With a regular magma supply over the long term, the stored magma in the chamber could be sufficient again to be released via regular (frequent) large explosive eruptions as recorded in the deep-sea basins, while more minor volcanic activity remains active in the middle section of the corridor (Figure 10c), including monogenetic volcanism and polygenetic volcanism. The polygenetic eruption in the middle section of the corridor might also release tephras into the sea basin. In the most recent part of this younger period, volcanism in the northeastern part of the corridor was again active (Figure 4).

6. Conclusion

[50] The Macolod Corridor is a Quaternary volcanic center in the southwestern part of Luzon Island in the Philippines. Two tephrostratigraphic records obtained from deep-sea cores to the west and east of Luzon Island have provided new constraints for the volcanic and tectonic evolution of the corridor, and in particular for the timing and spatial configuration of the steepening of the subducted slab. Temporal variations in the volcanic activity in the corridor and the spatial configuration of volcanoes reflect changes in the dynamics of the subducting South China Sea crust in the region.

[51] The results of this study show that large explosive eruptions characterize the northeastern section of the corridor prior to ~1400 ka, and the southwestern section since 478 ka. A relatively quiet intervening period from 1355 to 478 ka was characterized by small monogenetic explosive and effusive eruptions and small polygenetic eruptions in the middle section of the corridor. The locus of large, explosive volcanic eruptions during the Quaternary has therefore migrated from the northeast to the southwest of the corridor during the period 1355 to 478 ka. Combining the marine tephrostratigraphies with published onshore chronological data and interpretations of volcanic-tectonic dynamics, the relatively quiet period recorded in the deep-sea cores defines the period of steepening of the subducted slab beneath the Macolod Corridor.

Acknowledgments

[52] The authors are indebted to M. T. Chen of the National Taiwan Ocean University, as well as the scientific party and crew of the *Marion Dufresne* for coring in the South China Sea and west Philippine Sea on the IMAGES-III cruise. We gratefully acknowledge helpful discussions with K. Y. Wei and T. F. Yang at National Taiwan University and C. S. Horng at Academia Sinica of Taiwan at several stages in the progress of this project. This research was supported by grants from the National Science Council of the Republic of China to C. H. Chen (NSC 94-2116-M-001-009 and NSC 95-2116-001-004). The detailed and constructive reviews of Ulrich Knittel, Pat Castillo, and one anonymous reviewer as well as suggestions by editor John Tarduno improved the paper, and these are gratefully acknowledged.

References

Andal, E. S., Jr., G. P. Yumul, E. L. Listanco Jr., R. A. Tamayo, C. B. Dimalanta, and T. Ishii (2005), Characterization of the Pleistocene volcanic chain of the Bicol Arc, Philippines: Implications for geohazard assessment, *Terr. Atmos. Oceanic Sci.*, *16*(4), 865–883.

Barmin, A., O. Melnik, and R. S. J. Sparks (2002), Periodic behavior in lava dome eruptions, *Earth Planet. Sci. Lett.*, *199*(1–2), 173–184, doi:10.1016/S0012-821X(02)00557-5.

Bautista, B. C., M. L. P. Bautista, K. Oike, F. T. Wu, and R. S. Punongbayan (2001), A new insight on the geometry of subducting slabs in northern Luzon, Philippines, *Tectonophysics*, *339*(3–4), 279–310, doi:10.1016/S0040-1951(01)00120-2.

Bernard, A., U. Knittel, B. Weber, D. Weis, A. Albrecht, K. Hattori, J. Klein, and D. Oles (1996), Petrology and geochemistry of the 1991 eruption products of Mount Pinatubo, in *Fire and Mud: Eruptions and Lahars of Mount Pinatubo, Philippines*, edited by C. G. Newhall and R. S. Punongbayan, pp. 767–797, Univ. of Wash. Press, Seattle.

Cardwell, R. K., B. L. Isacks, and D. E. Karig (1980), The spatial distribution of earthquakes, focal mechanism solutions, and subducted lithosphere in the Philippine and northeastern Indonesian islands, in *The Tectonic and Geologic Evolution of Southeast Asian Seas and Islands: Part 1*, *Geophys. Monogr. Ser.*, vol. 23, edited by D. E. Hayes, pp. 1–35, AGU, Washington, D. C.

Castillo, P. R., and C. G. Newhall (2004), Geochemical constraints on possible subduction components in lavas of Mayon and Taal volcanoes, southern Luzon, Philippines, *J. Petrol.*, *45*(6), 1089–1108, doi:10.1093/petrology/egh005.

Castillo, P. R., and R. S. Punongbayan (1996), Petrology and Sr, Nd and Pb isotopic geochemistry of Mt. Pinatubo volcanic rocks, in *Fire and Mud: Eruptions and Lahars of Mount Pinatubo, Philippines*, edited by C. G. Newhall and R. S. Punongbayan, pp. 799–805, Univ. of Wash. Press, Seattle.

Catane, S., T. Ui, M. B. Arpa, H. B. Cabria, and H. Taniguchi (2004), Potential hazards from the youngest explosive eruptions of Laguna caldera to metropolitan Manila, Philippines, *Eos Trans. AGU*, *85*(28), West. Pac. Geophys. Meet. Suppl., Abstract V33A-89.

Catane, S. G., H. Taniguchi, A. Goto, A. P. Givero, and A. A. Mandanas (2005), *Explosive Volcanism in the Philippines*, *CNEAS Monogr. Ser.*, vol. 18, 131 pp., Cent. for North East Asian Stud., Tohoku Univ., Sendai, Japan.

de Boer, J., L. A. Odom, P. C. Ragland, F. G. Snider, and N. R. Tilford (1980), The Bataan orogene: Eastward subduction, tectonic rotations, and volcanism in the western Pacifics (Philippines), *Tectonophysics*, *67*(3–4), 251–282, doi:10.1016/0040-1951(80)90270-X.

Defant, M. J., and P. C. Ragland (1988), Recognition of contrasting magmatic processes using SB-systematics: An example from the western Central Luzon arc, the Philippines, *Chem. Geol.*, *67*(3–4), 197–208, doi:10.1016/0009-2541(88)90128-3.

Defant, M. C., J. de Boer, and D. Oles (1988), The western central Luzon volcanic arc, the Philippines: Two arcs divided by rifting?, *Tectonophysics*, *145*(3–4), 305–317, doi:10.1016/0040-1951(88)90202-8.

Defant, M. J., D. Jacques, R. C. Maury, J. de Boer, and J. L. Joron (1989), Geochemistry and tectonic setting of the Luzon arc, Philippines, *Geol. Soc. Am. Bull.*, *101*(5), 663–672, doi:10.1130/0016-7606(1989)101<0663:GATSOT>2.3.CO;2.

Defant, M. J., R. C. Maury, J. L. Joron, M. D. Feigenson, J. Leterrier, H. Bellon, D. Jacques, and M. Richard (1990), The geochemistry and tectonic setting of the northern section of the Luzon arc (the Philippines and Taiwan), *Tectonophysics*, *183*(1–4), 187–205, doi:10.1016/0040-1951(90)90416-6.

Defant, M. J., R. C. Maury, E. M. Ripley, M. D. Feigenson, and D. Jacques (1991), An example of island arc petrogenesis: Geochemistry and petrology of the southern Luzon arc, Philippines, *J. Petrol.*, *32*(3), 455–500.

Delfin, F. G., Jr., C. Panem-Conrado, and M. J. Defant (1993), Eruption history and petrochemistry of the Bulusan volcanic complex, implications for the hydrothermal system and volcanic hazards of Mount Bulusan, Philippines, *Geothermics*, *22*(5–6), 417–434, doi:10.1016/0375-6505(93)90029-M.

Denlinger, R., and R. P. Hoblitt (1999), Cyclic eruptive behavior of silicic volcanoes, *Geology*, *27*(5), 459–462, doi:10.1130/0091-7613(1999)027<0459:CEBOSV>2.3.CO;2.

Dickinson, W. R. (1975), Potash-depth (K-h) relations in continental margin and intra-oceanic magmatic arcs, *Geology*, *3*, 53–56, doi:10.1130/0091-7613(1975)3<53:PKRICM>2.0.CO;2.

Divis, A. F. (1980), The petrology and tectonics of recent volcanism in the central Philippine Islands, in *The Tectonic and Geologic Evolution of Southeast Asian Seas and Islands: Part 1*, *Geophys. Monogr. Ser.*, vol. 23, edited by D. E. Hayes, pp. 127–144, AGU, Washington, D. C.

DuFrane, S. A., Y. Asmerom, S. B. Mukasa, J. A. Morris, and B. Dreyer (2006), Subduction and melting processes inferred from U-Series, Sr-Nd-Pb isotope, and trace element data, Bataan and Bicol arcs, Philippines, *Geochim. Cosmochim. Acta*, *70*(13), 3401–3420, doi:10.1016/j.gca.2006.04.020.

Förster, H., D. Oles, U. Knittel, M. C. Defant, and R. C. Torres (1990), The Macolod Corridor: A rift crossing the Philippine island arc, *Tectonophysics*, *183*(1–4), 265–271, doi:10.1016/0040-1951(90)90420-D.

Hamburger, M. W., R. K. Cardwell, and B. L. Isacks (1983), Seismotectonics of the northern Philippine island arc, in *The Tectonic and Geologic Evolution of Southeast Asian Seas and Islands: Part 2*, *Geophys. Monogr. Ser.*, vol. 27, edited by D. E. Hayes, pp. 1–22, AGU, Washington, D. C.

Horng, C. S., M. Y. Lee, H. Palike, K. Y. Wei, W. T. Liang, Y. Iizuka, and T. Torii (2002), Astronomically calibrated ages for geomagnetic reversals within the Matuyama chron, *Earth Planets Space*, *54*, 679–690.

Huang, F., and C. C. Lundstrom (2007), ^{231}Pa excesses in arc volcanic rocks: Constraint on melting rates at convergent margins, *Geology*, *35*(11), 1007–1010, doi:10.1130/G23822A.1.

Huang, I. H. (2003), Tephra studies of the Core MD972143, western Philippine Sea, M.S. thesis, 92 pp., Dep. of Geosci., Natl. Taiwan Univ., Taipei, Taiwan.

Jellinek, A. M., and D. J. DePaolo (2003), A model for the origin of large silicic magma chambers: Precursors of caldera-forming eruptions, *Bull. Volcanol.*, *65*(5), 363–381, doi:10.1007/s00445-003-0277-y.

Kincaid, C., and R. W. Griffiths (2004), Variability in flow and temperatures within mantle subduction zones, *Geochem. Geophys. Geosyst.*, *5*, Q06002, doi:10.1029/2003GC000666.

Knittel, U., and M. J. Defant (1988), Sr isotopic and trace element variations in the Oligocene to Recent igneous rocks from the Philippine island arc: Evidence for Recent enrichment in the sub-Philippine mantle, *Earth Planet. Sci. Lett.*, *87*(1–2), 87–99, doi:10.1016/0012-821X(88)90066-0.

Knittel, U., and D. Oles (1995), Basaltic volcanism associated with extensional tectonics in the Taiwan-Luzon island arc: Evidence for non-depleted sources and subduction zone enrichment, in *Volcanism Associated With Extension at Consuming Plate Margins*, edited by J. L. Smellie, *Geol. Soc. Spec. Publ.*, *81*, 77–93.

Knittel, U., M. J. Defant, and I. Raczek (1988), Recent enrichment in the source region of arc magmas from Luzon island, Philippines: Sr and Nd isotopic evidence, *Geology*, *16*(1), 73–76, doi:10.1130/0091-7613(1988)016<0073:REITSR>2.3.CO;2.

Knittel, U., A. G. Trudu, W. Winter, T. Y. Yang, and C. M. Gray (1995), Volcanism above a subducted extinct spreading center: A reconnaissance study of the North Luzon Segment of the Taiwan-Luzon Volcanic Arc (Philippines), *J. Southeast Asian Earth Sci.*, *11*, 95–109, doi:10.1016/0743-9547(94)00039-H.

Knittel, U., E. Hegner, M. Bau, and M. Satir (1997), Enrichment processes in the sub-arc mantle: A Sr-Nd-Pb isotopic and REE study of primitive arc basalts from the Philippines, *Can. Mineral.*, *35*, 327–346.

Knittel-Weber, C., and U. Knittel (1990), Petrology and genesis of the volcanic rocks on the eastern flank of Mount Malinao, Bicol arc (southern Luzon, Philippines), *J. Southeast Asian Earth Sci.*, *4*, 267–280, doi:10.1016/0743-9547(90)90002-U.

Ku, Y. P., C. H. Chen, C. G. Newhall, S. R. Song, T. F. Yang, Y. Iizuka, and J. McGeehin (2008), Determining an age for the Inararo Tuff eruption of Mt. Pinatubo, based on correlation with a distal tephra layer in Core MD97-2142, South China Sea, *Quat. Int.*, *178*(1), 138–145, doi:10.1016/j.quaint.2007.02.025.

Lee, M. Y. (2000), Pliocene-Pleistocene event stratigraphy in the western Pacific marginal seas: Case studies of Australa-

sian microtektite, geomagnetic reversal and volcanic episodicity, Ph.D. thesis, 141 pp., Dep. of Geosci., Natl. Taiwan Univ., Taipei, Taiwan.

Listanco, E. L. (1994), Space-time patterns in the geologic and magmatic evolution of calderas: A case study at Taal Volcano, Philippines, Ph.D. thesis, 184 pp., Earthquake Res. Inst., Univ. of Tokyo, Tokyo.

Luhr, J. F., and W. G. Melson (1996), Mineral and glass compositions in June 15, 1991, pumices: Evidence for dynamic disequilibrium in the dacite of Mount Pinatubo, in *Fire and Mud: Eruptions and Lahars of Mount Pinatubo, Philippines*, edited by C. G. Newhall and R. S. Punongbayan, pp. 733–750, Univ. of Wash. Press, Seattle.

Marchadier, Y., and C. Rangin (1990), Polyphase tectonics at the southern tip of the Manila trench, Mindoro-Tablas islands, Philippines, *Tectonophysics*, *183*(1–4), 273–287, doi:10.1016/0040-1951(90)90421-4.

McDermott, F., M. J. Defant, C. J. Hawkesworth, R. C. Maury, and J. L. Joron (1993), Isotope and trace element evidence for three component mixing in the genesis of the North Luzon arc lavas (Philippines), *Contrib. Mineral. Petrol.*, *113*(1), 9–23, doi:10.1007/BF00320828.

McDermott, F., F. G. Delfin, M. J. Defant, S. Turner, and R. Maury (2005), The petrogenesis of volcanics from Mt. Bulusan and Mt. Mayon in the Bicol arc, the Philippines, *Contrib. Mineral. Petrol.*, *150*(6), 652–670, doi:10.1007/s00410-005-0042-7.

Miklius, A., M. F. Flower, J. P. Huijsmans, and P. Castillo (1991), Geochemistry of lavas from Taal volcano, southwestern Luzon, Philippines: Evidence for multiple magma supply systems and mantle source heterogeneity, *J. Petrol.*, *32*(3), 593–627.

Mukasa, S. B., M. F. J. Flower, and A. Miklius (1994), The Nd-, Sr- and Pb-isotopic character of lavas from Taal, Laguna de Bay and Arayat volcanoes, southwestern Luzon, Philippines: Implications for arc magma petrogenesis, *Tectonophysics*, *235*(1–2), 205–221, doi:10.1016/0040-1951(94)90024-8.

Nakagawa, M., and T. Ohba (2002), Minerals in volcanic ash 1: Primary minerals and volcanic glass, *Global Environ. Res.*, *6*(2), 41–51.

Oles, D. (1991), Geology of the Macolod Corridor intersecting the Bataan-Mindoro island arc, the Philippines, *Proj. Fo 53/16–1 to 2*, Philipp. Inst. of Volcanol. and Seismol., Dep. of Sci. and Technol., Quezon City, Philippines.

Pouclet, A., M. Pubellier, and P. Spadea (1991), Volcanic ash from Celebes and Sulu Sea basins off the Philippines (Leg 124): Petrography and geochemistry, *Proc. Ocean Drill. Program Sci. Results*, *124*, 467–487.

Rickwood, P. C. (1989), Boundary lines within petrologic diagrams which use oxides of major and minor elements, *Lithos*, *22*(4), 247–263, doi:10.1016/0024-4937(89)90028-5.

Scandone, R., K. V. Cashman, and S. D. Malone (2007), Magma supply, magma ascent and the style of volcanic eruptions, *Earth Planet. Sci. Lett.*, *253*(3–4), 513–529, doi:10.1016/j.epsl.2006.11.016.

Sudo, M., E. D. Listanco, N. Ishikawa, T. Tagami, H. Kamata, and Y. Tatsumi (2000), K-Ar dating of the volcanic rocks from Macolod corridor in southwestern Luzon, Philippines: Toward understanding of the Quaternary volcanism and tectonic, *J. Geol. Soc. Philipp.*, *55*(1–2), 89–104.

Tatsumi, Y., S. Eggins (Eds.) (1995), *Subduction Zone Magmatism*, 211 pp., Blackwell Sci., Cambridge, Mass.

Torres, R. C., S. Self, and R. S. Punongbayan (1995), Attention focuses on Taal: Decade volcano of the Philippines, *Eos Trans. AGU*, *76*(24), 241–247, doi:10.1029/95EO00137.

Tsai, R. H. (2000), Size and geochemical analysis of tephra layers in Core MD972142, South China Sea and their implications, M.S. thesis, 59 pp., Dep. of Geosci., Natl. Taiwan Univ., Taipei, Taiwan.

Vogel, T. A., T. P. Flood, L. C. Patino, M. S. Wilmot, R. P. R. Maximo, C. B. Arpa, C. A. Arcilla, and J. A. Stimac (2006), Geochemistry of silicic magmas in the Macolod Corridor, SW Luzon, Philippines: Evidence of distinct, mantle-derived, crustal sources for silicic magmas, *Contrib. Mineral. Petrol.*, *151*(3), 267–281, doi:10.1007/s00410-005-0050-7.

Wei, K. Y., T. Q. Lee, and the Scientific Party of ImAGES III/MD106-IPHIS Cruise (Leg II) (1998), Late Pleistocene volcanic tephra layers in Core MD972142, offshore from northwestern Palawan, South China Sea: A preliminary report, *Terr. Atmos. Oceanic Sci.*, *9*(1), 143–152.

Wei, K. Y., T. C. Chiu, and Y. G. Chen (2003), Toward establishing a maritime proxy record of the east Asia summer monsoons for the Late Quaternary, *Mar. Geol.*, *201*(1–3), 67–79, doi:10.1016/S0025-3227(03)00209-3.

Wolfe, J. A. (1981), Philippine geochronology, *J. Geol. Soc. Philipp.*, *35*(1), 1–30.

Wolfe, J. A., and S. Self (1983), Structural lineaments and Neogene volcanism in southwestern Luzon, in *The Tectonic and Geologic Evolution of Southeast Asian Seas and Islands: Part 2*, *Geophys. Monogr. Ser.*, vol. 27, edited by D. E. Hayes, pp. 151–172, AGU, Washington, D. C.

Yang, T. F., T. Lee, C. H. Chen, S. N. Cheng, U. Knittel, R. S. Punongbayan, and A. R. Rasdas (1996), A double island arc between Taiwan and Luzon: Consequence of ridge subduction, *Tectonophysics*, *258*(1–4), 85–101, doi:10.1016/0040-1951(95)00180-8.